Association of ^{241}Am and ^{137}Cs in finer size-fractioned saltmarsh sediments from north-west England, UK and potential health risk to coastal populations.

Rubina Rahman[1,2*] and Andrew J. Plater[1]

[1]Department of Geography, University of Liverpool, Roxby Building, L69 7ZT, UK.

[2]Department of Physics, Jahangirnagar University, Savar, Dhaka-1342, Bangladesh.

[*] Corresponding author: rrahman@liv.ac.uk; rrahman@juniv.edu

Abstract:

This study provides an in-depth analysis of the relationship between radionuclide and particle size-class abundance through an investigation of radionuclide distribution in finer sediments within surface core samples collected from two contaminated upper saltmarsh areas of the Dee estuary and Biggar marsh in North-West England. The particle size fractionation (PSF) analysis was carried out following gravitational settling and pipette method to separate all samples into six size-fractioned groups ranging from 63 to <2 µm (very coarse silt to clay), and radioactivity analysis was performed using a well-type High Purity Germanium (HPGe) detector. The highest ^{241}Am and ^{137}Cs activities in PSF samples were found to be 291 ± 5 and 2071 ± 16 Bq kg^{-1}, respectively, for the Dee estuary saltmarsh and 3832 ± 14 and 4840 ± 23 Bq kg^{-1}, respectively, for Biggar saltmarsh and found in the clay fractions for both sites. Correlation of radioactivity concentration data of three size groups ranging from 63 to <2 µm (very coarse silt to clay) confirms a strong and increasing association of radioactivity with fine particles from coarse to fine clay-size particles. Also, examination of textural and radionuclide data of all bulk core and size-fractioned samples revealed that upper saltmarshes are made up of both contaminated and uncontaminated sediments. Furthermore, the annual outdoor external effective dose range for all short core data (0.001 to 0.11 mSv y^{-1}) and for PSF sample data (0.001 to 0.08 mSv y^{-1}) reveal that some values exceed the world average value of 0.07 mSv y^{-1} as reported in UNSCEAR [43], for outdoor, which are non-negligible. Thus, the total annual external effective dose associated with existing contaminated saltmarsh sediments represents a possible health risk to saltmarsh users and coastal populations living nearby these saltmarshes.

Key words: Saltmarsh; sediments; radionuclides; Size-fractionation analysis; fine-particles;

HPGe detector; Gamma-ray spectrometry.

Introduction

Radionuclides present in coastal estuary and saltmarsh sediments are subject to several natural and geological processes where particle size plays an important role. Sedimentation in estuaries is normally viewed as a continuous process controlled by inputs of fluvial and marine materials, which migrate in response to tidal circulation and deposition of the fine 'mud' fraction occurs as a result of the interaction between currents, tides and salinity [1]. Thus, estuaries represent a restricted exchange environment that can act as a sink or source of sediment and sediment-associated contaminants discharged into the aquatic environment [2]. Saltmarshes are a common feature of an estuary and are usually found within temperate and high latitudes along the coast where the wave action and other disturbance forces are relatively low. Saltmarshes therefore develop along low wave-energy coastlines, usually in estuaries, river mouths, back-barrier lagoons and bays, and deltas. As a result of low-energy tidal currents, saltmarshes sediments generally become finer onshore towards the upper marsh areas [3-5].

The major source of anthropogenic radionuclides found in several UK coastal and Irish Sea saltmarshes is the Sellafield waste reprocessing facility, which has been discharging radionuclides like ^{134}Cs, ^{137}Cs, ^{241}Pu, ^{241}Am, ^{3}H, ^{14}C, ^{90}Sr, ^{99}Tc etc. as regulated radioactive wastes under license into the Irish Sea since 1952 onwards and have declined after mid-1980s, from the peak releases in mid-1970s [6-14]. Another minor source of anthropogenic radionuclides input, mainly ^{137}Cs, into the Irish Sea saltmarshes is from atmospheric testing of nuclear weapons carried out from 1945 to 1980, and accidents that occurred at nuclear power plants such as the incident at the Chernobyl nuclear power plant in 1986 and the accident at Windscale in the United Kingdom in 1957.

Among all Sellafield radionuclides that are found in UK saltmarshes, particle-reactive ^{241}Am (half-life: 432.7 y) tends to adsorb rapidly onto sediment following discharge

whilst the alkali metal ^{137}Cs (half-life: 30.2 y) is found in saline water and can undergo wider dispersion by tidal currents. Importantly, both radionuclides exhibit preferential sorption with respect to fine grained sediment [15,16]. Moreover, it is well established from previous studies that radionuclides have a high affinity for fine particles [14,16-18]. Hence, based on these findings, particle size fractionation analysis has been undertaken to observe ^{137}Cs and ^{241}Am radioactivity levels in six finer grain size groups (63 - <2 μm) particularly from organic- and mineral-rich surface saltmarsh box core samples of 10 cm depth, from upper saltmarshes of two saltmarshes (Figure 1) namely the Dee estuary (Parkgate and Moorside) and Biggar marsh on Walney Island, UK. The study was undertaken with a view to identify the dominant particle size which is most responsible for associated radioactivity levels from Sellafield-derived radionuclides within these upper saltmarshes.

The relationship between radionuclide content and particle size-class abundance was explored with a view to investigating the potential health risk from the estimated annual effective dose associated with existing finer particles of contaminated saltmarsh sediments those are associated with highly active ^{241}Am and ^{137}Cs. Hence, radionuclide activities were determined in particle size fractionated sediment samples from short box core samples collected from the upper marshes of both sites.

Moreover, both saltmarshes now appear to be approaching a quasi-equilibrium stage where the saltmarsh accretion is limited by the tidal level, and then there is considerable potential that both marshes may be eroded [14,19-20]. As a consequence, re-suspended mud will increase in the tidal sediment budget which contains accumulated pollutants (e.g. metals, radionuclides etc.) from years past, many of which are now banned or strictly regulated due to their environmental and human health impacts [7, 9, 14]. Hence, in present study the investigation was performed in three steps: in first step the Sellafield-derived ^{241}Am and ^{137}Cs concentrations were determined and measured in sediments from two saltmarshes (Figure 1) of north-west England. In second step, investigation was carried out to find out the association of both ^{241}Am and ^{137}Cs with attached fine sediments according to their concentrations within individual finer grain size particles. In

third step, radiological assessment was examined to investigate potential exposure health risks from both analysed radionuclides to saltmarsh users and coastal population from both collected short core total radionuclide data and radionuclide concentrations in each size-fractioned sediment sample for all short cores. The investigation aimed to provide an overall understanding of health risk issues to saltmarsh users and coastal populations from existing radionuclides attached finer surface marsh sediments as well as redistributed historic highly active radionuclides attached to core sediments that may arise from saltmarsh erosion or through human interventions.

2. Methodology

2.1 Sample collection and particle size fractionation

A total of eleven surface box core samples (10 cm length) were collected from the upper saltmarsh areas of the Dee estuary (seven cores) and Biggar marsh (four cores) saltmarshes (Figure 1). The upper saltmarsh area was chosen in this study as the sub-surface peak of the depth profile of Sellafield-derived radionuclides were found just under 5-20 cm depths from these sites, [21] and they were found to be rich in fine sediments [14]. Prior to size-fractionation analysis, the particle size distribution (PSD) curves of all samples (Figure 2) were examined to confirm the existence of fine sediments. The PSD curves were obtained through laser granulometric measurements and without any H_2O_2 (hydrogen peroxide) digestion process to avoid any leaching of surface-bound radionuclide. Hence, both organic and mineral matter was included in particle size fractionation (PSF) analysis.

The particle size fractionation (PSF) analysis was carried out following a gravitational settling pipette method and using Stoke's law to separate all surface core samples into six size-fractioned groups of 63 - >31, 31- >6, 16 - >8, 8 - >4, 4 - >2 and 2 to <2 μm, i.e., from the mud size-class range (very coarse silt to clay) [14, 18, 22-24]. During each PSF procedure particle dispersion was carried out using lab-produced equivalent sea water (pH 7.7) and each size fraction was obtained through calculating settling times, based on

the assumption that the density of the solid is 2.65 g cm^{-3}, equivalent to that of quartz, as followed in other studies [14, 16, 18, 24-25].

The uncertainties in the particle size of fractionated size classes obtained from this settling procedure was determined using a Beckman Coulter LS200 laser diffraction particle size analyser, as this analyser has been found to be accurate and precise in its measurement of particle size [26]. The LS200 can measure particles with diameters from 0.4μm to 2000μm through laser light of 750 nm wavelength. The composite diffraction pattern is measured by 126 detectors placed at angles at approximately 35 degrees from the optical axis in the present study. All data from the laser granulometer were processed using well-established software: GRADISTAT (version 4.0), developed by Blott [27]. This is a rapid analytical program to determines and present grain size statistics for any of the standard particle size measurement techniques. The percentages of sediment detected in size classes derived from the laser granulometer are then calculated for mean, mode(s), sorting (standard deviation), skewness, kurtosis, and a range of cumulative percentile values. In the program, the method of moments is used to calculate statistics *arithmetically* (based on a normal distribution with metric size values), *geometrically* (based on a log-normal distribution with metric size values) and *logarithmically* (based on a log-normal distribution with phi size values), following the terminology and formulae suggested by Krumbein and Pettijohn [28]. The program also provides a physical description of the textural class after Folk [29]. Specified values are then extracted from the cumulative percentage curve using a linear interpolation between adjacent known points on the curve as shown in Figure 3 and using formulae as Eq. (1-3) below:

$$\text{Graphic standard deviation or sorting } (\sigma_I) = \frac{\phi_{84} - \phi_{16}}{4} + \frac{\phi_{95} - \phi_5}{6.6} \quad (1)$$

$$\text{Graphic skewness } (Sk_I) = \frac{\phi_{16} + \phi_{84} - 2\phi_{50}}{2(\phi_{84} - \phi_{16})} + \frac{\phi_5 + \phi_{95} - 2\phi_{50}}{2(\phi_{95} - \phi_5)} \quad (2)$$

Graphic kurtosis (K_G) = $$\frac{\phi_{95} - \phi_5}{2.44(\phi_{75} - \phi_{25})} \quad (3)$$

In this study all particle size data are expressed as logarithmic Folk and Ward [30] graphical measures in φ units. For more intuitive understanding of grain size, these results were also converted and represented as μm (micrometer or micron) in present study.

2.2 Accuracy of fractionation procedure analysis

Particle size fractionation through gravimetric settling procedures is well established. Though most previous studies [16, 31] have paid little attention to the potential effect of inefficient size-fractionation on radionuclide concentration in grain size fractions, Clifton et al. [18] illustrated the importance of questioning the efficiency and accuracy of size-fractionation procedures. Thus, size fractioned samples in this study were analysed by laser granulometry on a regular basis during the process to cross-check the precision of the gravimetric methods and associated procedures. Figure 4 shows example plots of the % volume distribution curves from the size fractions (ranging between 63 and <2 μm) obtained in this study through gravimetric fractionation procedures for two upper saltmarsh short box core samples D1 (Dee estuary) and B1 (Biggar marsh). The modal peaks in successive size fractions can easily be identified from both plots, where each modal peak is separated by at least one phi unit. It is also identified that with the progressive increase of the modal grain size (decreasing φ value or increasing μm), the degree of sorting improves (reduced dispersion either side of the mean grain size) but the fine skew increases (increasing excess of finer grain sizes in the distribution). Throughout the process, particle dispersion was carried out using lab-produced equivalent sea water (pH 7.7) and without any ultrasound particle dispersion, thus avoiding any enhanced desorption or loss from the finer grains, as described in previous study [23], very few coarse sub-modes arising from the flocculation of fines were apparent (Figure 4).

It is often assumed that the coarser sub-modes in the finer fractions may be flocculated fine grains or due to the influence of low density coarser organic particles [23]. However,

the presence of a flocculated dense layer of suspended sediment overlain by a clear fluid zone which is usually indicative of this process as reported by Allen [32], was not observed during the experiment. Hence, it is considered that the presence of the coarser component within the size fractioned samples in this study is a reflection of the effects of variable shape of the measured particles, as discussed in Barbanti and Bothner [23]. Moreover, it is also observed that there are no long coarse tails in the size fraction distribution curves, as was observed for the results from the same size fractions measured by Clifton et al. [18]. Hence, the gravimetric methods and procedures in the present study worked precisely in terms of their upper limit.

In terms of uncertainly in the particle size fractionation, our analysis demonstrates that a high proportion of the grain population is situated within the designated size range (Figure 4). This does not mean that finer and coarser grains are excluded, indeed one expects this from the settling methodology in relation to variability in particle density and shape. Essentially, as the finer size fractions tend to have a greater proportion of platy grains of clay minerals, there is a greater spread of sizes in the population, with a preference for the finer particles. The cited particle size ranges are therefore considered as position of the mean particle size for that fraction but with an increasing standard deviation and fine skew for progressively finer fractions in this study. The cited 1φ difference in the fractionated particle sizes is further supported by the evident size separation of the modal grain sizes (Figure 4).

2.3 *Gamma-ray spectrometry analysis*

For both saltmarsh sites, the activity concentrations of gamma ray emitting radioisotopes from all

size-fractioned samples (63 - <2 μm) from short cores were measured and analysed using a high-resolution well-type HPGe detector (ERRC, University of Liverpool) coupled with Multi-Channel Analyzer (MCA). The well detector had a crystal length of 6.08 cm and diameter of 5.52 cm, effective well depth of 4.42 cm and well diameter of 1.65 cm,

operated with an electric field of 3000 V with negative bias. The resolution for the well detector was of 1.89 at 59.7 keV and 2.45 at 1332 keV. The detector configuration was set in the 40-2000 keV range, for detecting photons. To avoid back scattering and reduce background activity, the detector was shielded by lead and copper sheets and all sample holders were of 0.5 cm diameter and 5 cm height. The counting time was set for 172800 s. The activity concentrations of ^{137}Cs and ^{241}Am were calculated through 661.66 keV and 59.7 keV, respectively. In this study, energy calibrations for the detector were conducted using NPRL ^{137}Cs and ^{241}Am calibrated point sources and detector was calibrated using NPL standard sources adsorbed onto a powdered resin base. The absolute efficiencies of the detectors were determined using calibrated sources and sediment samples of known activity. Corrections were made for the effect of self-absorption of low energy γ-rays within the sample [33].

2.3.1 Radionuclide Activity calculation

The activity concentrations (A) of the investigated radionuclides and the efficiency (ε_γ) of the well-type HPGE detector used in this study were calculated using Eq. (4) below [34-37]:

$$\mathrm{A} = \frac{N}{\varepsilon_\gamma \times \rho_\gamma \times T_s \times M_s} \quad (4)$$

where, A represents the specific activity in Bq kg^{-1}, N represents the net number of counts under the characteristic photo-peak, ε_γ is the efficiency of the detector at the corresponding gamma-ray energy, ρ_γ represents the branching ratio, T_s is the counting time in seconds and M_s stands for the weight of the sample in kilograms (kg). For the gamma-ray measurement system, the minimum detectable activity concentration (MDAC) was determined using the Eq. (5) as reported in [37]:

$$\mathrm{MDAC} = \frac{\mathrm{K}_\alpha \times \sqrt{\mathrm{B}}}{\epsilon_\gamma \times \rho_\gamma \times \mathrm{T_s} \times \mathrm{M_s}} \quad (5)$$

where K_α is the statistical coverage factor having a value of 1.64 (at the 95% confidence

level), B is the number of background counts for the corresponding radionuclide, ε_γ, ρ_γ, T_s, and M_s (in kg) have their usual meaning similar to Eq. (1). The MDAC values for the investigated radionuclides in this study were found to be 0.10 Bq kg^{-1} and 0.04 Bq kg^{-1}, for ^{137}Cs and ^{241}Am, respectively. The uncertainty of the measured activity concentration was derived using following Eq. (6) below [37]

$$\sigma = \sqrt{\left[\frac{N_s}{T_s^2} + \frac{N_b}{T_b^2}\right]} \quad (6)$$

where N_s is the measured counts in time T_s and N_b is the background counts in time T_b. The standard deviation (± 2σ), in CPS, was then transformed into activity concentration in Bq kg^{-1}.

2.3.2 External annual Effective dose calculation

For different saltmarsh users such as Farmer, Walker/Dog walker, Ranger, Birdwatcher, Herdsman etc., the external effective dose rates (for adult) were calculated using the Hunt semi-infinite source model equation (which is used in CUMBRIA77/DOSE77 assessments) [21,38-39], as Eq. (7) below:

$$\text{External Effective Dose (Sv } y^{-1}) = (A_n \times V_n \times 2.88 \times 10^{-4}) \times O_h \times C \quad (7)$$

where A_n is the activity concentration of the radionuclide 'n' in saltmarsh sediment (Bq kg^{-1}), V_n is the energy of the radiation emitted by the nuclide 'n' (MeV), O_h is the annual occupancy hours (h y^{-1}) and C is the conversion factor, 8.6 × 10^{-7} (Sv mG^{-1}) for converting air kerma or absorbed dose-to-air to effective dose equivalent [39, 40]. The annual occupancy hours used in this study are adopted from other studies based on fieldwork interviews [41, 42] and were taken as 312 h y^{-1}, for minimum annual occupancy and 730 h y^{-1}, for maximum annual outdoor occupancy, with a consideration of 10% uncertainty on the estimated occupancy values. Thus, for both ^{137}Cs and ^{241}Am, the total uncertainties in the annual external effective dose only considered uncertainties

of activity concentration and annual occupancy neglecting uncertainties from V_n for gamma.

3. Results

3.1 Radionuclide and textural gross data of short core samples

Table 1 summarises the range of radionuclide activities and grain size characteristics in selected surface box core samples. It is seen that the gross ^{241}Am and ^{137}Cs activities observed in the core samples from the Dee estuary (Parkgate and Moorside) range from 88 to 269 Bq kg^{-1} and 306 to 1309 Bq kg^{-1}, respectively. For Biggar saltmarsh, the gross ^{241}Am and ^{137}Cs activities range from 925 to 2581 Bq kg^{-1} and 474 to 1980 Bq kg^{-1}, respectively. Again, ^{241}Am activity concentration is much higher for Biggar marsh compared to the Dee estuary saltmarshes, whereas ^{137}Cs activity concentrations are quite comparable. All samples from both marshes are rich in clay (15-22%) to silt (above 70%) with very little sand (0-7%) (Figure 2). For both sites, the uncertainty for ^{241}Am and ^{137}Cs activity ranged between 2 and 10%, and for the measured % size class particles the approximate estimated uncertainties were estimated to be 1% from observation of replicated samples (Table 1).

3.2 Radionuclide data for size fractions

Tables 2-3 summarise the radionuclide activity data derived from analysis of measured particle size fractions whereas Figures 5 and 6 illustrate these data for cores D1, D2, D3, D4, D5, D6 and D7 for the Dee estuary and B1, B2, B3 and B4 for the Biggar marsh, respectively.

For the Dee estuary, it is seen from Figures 5a-5g that for all core samples there are considerably elevated ^{137}Cs activities in finer particle size fractions and a consistent decreasing trend in activities in coarser fractions. A similar trend is also present for ^{241}Am but with much lower activities than ^{137}Cs. The highest ^{241}Am and ^{137}Cs activities found in the individual size fractions were 291 ± 5 and 2071 ± 16 Bq kg^{-1} (indicated in bold font in Table 2), respectively, in the clay (2 - <2 μm) fractions upper saltmarsh core D2. A clearer understanding of the radionuclide activities in the finer particle size

fractions can be obtained when the mean ^{241}Am and ^{137}Cs activities of these measured size fractions are scrutinized across three grain-size classes: very coarse silt to coarse silt, medium silt to fine silt and very fine silt to clay. The value within the bracket shows the corresponding mean % abundance of total sample volume in three size class fractions (Table 2).

For Biggar saltmarsh, similarly elevated activity concentrations in the finer particle size fractions and a consistent decreasing trend in activities in coarser fraction are present for both ^{241}Am and ^{137}Cs and in all core samples (Figure 6a-6d). These data indicate the presence of ^{241}Am levels in the Biggar marsh core samples. The highest ^{241}Am and ^{137}Cs activities observed in each individual size fraction were 3832 ± 14 and 4840 ± 23 Bq kg^{-1} (in bold font in Table 3), respectively, in clay (2 - <2 μm) fractions from core B2.

3.3 Effective dose rate estimation and Health risk assessment

Table 4a shows the outdoor annual external effective dose for total radionuclide (^{241}Am and ^{137}Cs) for collected short cores in this study. For ^{241}Am, the annual outdoor external effective doses for total radionuclide of seven short cores of the Dee estuary upper saltmarshes ranged from 0.001 to 0.002 mSv y^{-1}, with a mean of 0.001 mSv y^{-1}, and for four cores from Biggar saltmarsh were found in range from 0.01 to 0.02 mSv y^{-1}, with a mean of 0.01 mSv y^{-1}. For ^{137}Cs, the annual outdoor external effective doses for total radionuclide of seven short cores of the Dee estuary upper saltmarshes ranged from 0.03 to 0.08 mSv y^{-1}, with a mean of 0.05 mSv y^{-1}, and for four cores from Biggar saltmarsh were found in range from 0.06 to 0.15 mSv y^{-1}, with a mean of 0.11 mSv y^{-1}.

On the other hand, Table 4b shows the outdoor annual external effective dose data of the mean activity of all PSF samples (63 - <2 μm) for all investigated short cores: seven from the Dee estuary and four from Biggar saltmarsh. For the PSF samples of the Dee estuary saltmarshes, the annual effective dose for ^{241}Am and ^{137}Cs, range from 0.001 to 0.0013 mSv y^{-1}, with a mean of 0.001 mSv y^{-1}, and 0.005 to 0.01 mSv y^{-1}, with a mean of 0.06 mSv y^{-1}, respectively. On the other hand, for Biggar saltmarshes, the annual effective

dose for ^{241}Am and ^{137}Cs, range from 0.03 to 0.08 mSv y^{-1}, with a mean of 0.01 mSv y^{-1}, and 0.05 to 0.11 mSv y^{-1}, with a mean of 0.08 mSv y^{-1}, respectively.

Furthermore, Figure 7a-7d shows the relative annual outdoor effective dose distribution due to total ^{241}Am and ^{137}Cs radionuclide contribution in the investigated short cores from the Dee estuary and Biggar upper saltmarsh areas. It is seen that For the Dee estuary, ^{137}Cs activity concentration (81%) is higher than ^{241}Am activity concentration (19%). On the other hand, though for the Biggar saltmarsh ^{241}Am activity concentration (56%) is high compared to^{137}Cs (44%) but the annual external effective dose contribution of ^{137}Cs (94%) is still higher than ^{241}Am (6%). Thus, for both marshes it is observed that ^{137}Cs is the major dose contributor.

Radiological data also reveal that for both the Dee estuary and Biggar saltmarshes, some values of the outdoor external annual effective dose for all short cores and radionuclide data of all PSF samples (from 63 - < 2 μm) exceed the world average value of 0.07 $mSvy^{-1}$ [43], for outdoor, which are non-negligeable.

3.4 Textural data of abundant size-fractions

Table 5 summarises the textural data of selected particle size-fractions (mud texture) available for the Dee estuary and Biggar saltmarsh cores. The data tabulated in Table 5 reveal that all upper saltmarsh cores from both sites fall into the mud textural group except for the D5 and D6 cores from the Dee estuary where the sediments fall into the sandy mud textural group. Also, the % in chosen grain size-class are above 90% to 100% for all 9 cores (D1-D4, D7, B1-B4). For the D5 and D6 cores, more than 80% falls into the chosen grain size-class and only 17% falls into fine sand-size group of grains. In relation to finer size classes, it is observed that for all the Dee estuary cores, except D5 and D6, the fine silts to clay grains make up 52-59 %, the medium silts are 19-21% and very coarse to coarse silts are 19-23 % of the total whereas for the D5 and D6 cores, these values range from 43 to 48 %, 14 to 15 % and 21 to 25%, respectively. The highest abundance of fine silts to clay is ca. 59 % in D1. On the other hand, for Biggar saltmarsh cores, the fine silts to clay grains make up 44-52 %, the medium silts are 18-21% and

very coarse to coarse silts are 23-28 % of the total**.** The highest abundance in the finer fraction component for Biggar saltmarsh is 52 % in B3.

3.4 Radionuclide content, LOI and size class abundance correlations

Further analyses have been done to examine correlations between the radionuclide content and organic carbon with the % abundance of measured grain size fractions in this study. Table 6 presents calculated rank correlation coefficients between radionuclide activity, % loss on ignition (LOI, as a proxy for organic carbon) and % abundance of selected particle size classes for both saltmarsh short core samples. No specific and significant (threshold P value assumed as 0.92) correlations are observed within these parameters, except in one case for the 6 - <7 % (medium silt) size-class from the Dee where a strong correlation between LOI and % abundance is observed. Moreover, a few data from both marshes exhibit weak positive correlations but they are not significant. Thus, the absence of significant correlations between ^{241}Am and ^{137}Cs activities and % abundance of size fractioned samples simply means that although high radionuclide activities have a strong affinity with finer grains, high proportions of finer sizes do not necessarily convert to higher activities. This is due potentially to dilution from unpolluted particles of the same class-size.

4. Discussions

4.1 Radionuclide data and grain size fractions

The consistency of increasing ^{241}Am and ^{137}Cs activities with decreasing grain size from both marshes according to three observed grain fractions: very coarse to coarse silts, medium to fine silts and fine silts to clay confirm that there are significant (Figure 8) correlations between increased activity and reduced grain size. However, the finest size fractions are not always associated with enhanced ^{241}Am activity to the same extent as found with respect to ^{137}Cs, and the lack of increased ^{241}Am activity in finer size fractions has also been observed by Clifton [44] which further supports this observation. The highest specific radionuclide activities in the <63 μm grain size fractions are also in

agreement with other findings from saltmarshes and Irish Sea sediments [11, 13, 15, 18, 44-46].

4.2. Implications for ^{241}Am and ^{137}Cs phase associations

The detailed examination of grain size data (Table 5) reveals that for both sites there are high % abundances of fine grains (63 - <2 μm) ranging between 93 and 100% within the bulk short core samples, and ^{241}Am and ^{137}Cs activities increase from coarser silts to finer particle sizes. Although the % abundance of fine grains are high there are no positive and significant (threshold P value of 0.92) rank correlations between the radionuclide activities, LOI (as a proxy for organic carbon content) and the % abundance of the size-fractions (Table 6). This means that the ^{241}Am and ^{137}Cs activity levels in all bulk core samples are a product of both contaminated and uncontaminated fine sediments. The less elevated particulate associated ^{241}Am activities (Figure 5-6) from both saltmarsh cores are not significantly influenced by the organic carbon contents (Table 6) which is opposite to observation of Clifton [18]. However, the lack of increases ^{241}Am activities in finer grains may point towards the influence of geochemical phases upon ^{241}Am adsorption which obscure the effect of a greater surface area available for radionuclide adsorption. Indeed, the association of ^{241}Am with sediment is still a subject to debate [47] as geochemistry may vary from one saltmarsh to other. Hence, to understand the geochemical behaviour of ^{241}Am with saltmarsh sediments, further detailed study is needed.

5. Conclusions

The present study determined the existence of highly active Sellafield derived ^{241}Am and ^{137}Cs in the Dee estuary and Biggar saltmarsh short core sediments. Also, particle size fractionation analysis was carried out for all short box core samples collected from upper marshes of both sites, and explored the relationship between radionuclide content and finer particle size-class abundance (63 - <2 μm). Finally, radiological assessment was carried out to investigate the potential health risk from these contaminated finer particles of saltmarsh sediments, associated with highly active ^{241}Am and ^{137}Cs. The study showed that there is a consistency of increasing ^{241}Am and ^{137}Cs activities with finer grains in

three observed size fractions: very coarse to coarse silts (63 - >16 μm), medium to fine silts (16 - >8 μm) and fine silts to clay (8 - >2 μm). Also, there are high % abundances of fine grains (63 - <2 μm), i.e % mud ranging between 93 and 100% within the bulk short core samples. However, whilst the % abundance of fine grains is high, there are no positive and significant correlations between the radionuclide activities, LOI (as a proxy for organic carbon content) and the % abundance of the fine size-fractions. Hence, it seems that the ^{241}Am and ^{137}Cs activity levels in all bulk core samples are a product of both contaminated and uncontaminated fine sediments. Finally, the radiological assessment showed that for both saltmarsh sites, ^{137}Cs is the main annual external effective dose contributor and some effective dose rate values exceed the world average value of 0.07 mSv y^{-1} [43] for outdoor and are non-negligible. Thus, it can be concluded that outdoor exposures from the existing ^{241}Am and ^{137}Cs in contaminated sediments of the Dee estuary and Biggar saltmarshes possess potential health risks to saltmarsh users and coastal population living nearby these saltmarshes.

Acknowledgements

The present research work was funded by Overseas Research Scholarship and University of Liverpool International Scholarship. The authors would like to thank Paul Nolan, Barbara Mauz and Peter Appleby for their advisory input during the research works.

Declaration of interests

The authors declare that they have no known competing financial interests or personal relationships that could have appeared to influence the work reported in this paper.

References

[1] J. McManus, Temporal and spatial variations in estuarine Sedimentation; Joint Estuarine and

Coastal Sciences Association-Estuarine Research Federation (ECSA-ERF) Symposium no.

2,

Estuaries **21** (4A), 622 (1998).

[2] M.P Rainey, A.N. Tyler, D.J. Gilvear, R.G. Bryant and P. McDonald, Remote Sensing of

Environ **86**, 480 (2003).

[3] L. A. Boorman, A. Garbutt and D. Barratt, The role of vegetation in determining patterns of

the accretion of saltmarsh sediment. In: Black, K.S., Paterson, D.M. and Cramp, A. (Eds.).

Sedimentary processes in the intertidal zone. Geological Society of London Special Publications **139**, 389 (1998).

[4] C.T. Friedrichs and J.E. Perry, J. of Coast. Res **27**, 7 (2001).

[5] R.G.D. Davidson-Arnott, D. Van Proosdij, J. Ollerhead.and L. Schostak, Geomorph **48** (1),

209 (2002).

[6] D.F. Jefferies, A. Preston and A.K. Steel, Mar Pollut Bull **4**,118 (1973).

[7] P.J.P. Bonnet, P.G. Appleby and F. Oldfield, Sci Tot Environ **70**, 215 (1988).

[8] P.J. Kershaw and A.J. Baxter, Sellafield as a source of radioactivity to the Barents

Sea. Proceedings of the Environmental Radioactivity in Arctic and Antarctic. NRPA, Osteras,

161 (1993).

[9] F. Oldfield, N. Richardson and P.G. Appleby, J. Environ Radioact **19** (1), 1 (1993).

[10] J. Gray, S.R. Jones and A.D. Smith, J. Radiolog Protec **2**, 99 (1995).

[11] J. Clifton, P. MacDonald, A. Plater and F. Oldfield, Water, Air and Soil Poll. **99**, 209

(1997).

[12] P.J. Kershaw, D.C. Denoon and D.S. Woodhead, J. Environ Radioact **44**, 191 (1999).

[13] M.E. Charlesworth, M. Service and C.E. Gibson, Sci Tot Environ **354**, 83 (2006).

[14] Rubina Rahman, PhD thesis. Radioactive pollution and potential redistribution, exposure

and health risks from Sellafield-contaminated saltmarshes in north-west England, UK

University of Liverpool, Liverpool, UK (2010).

[15] R.C. Carpenter, P.J. Burton, L.P. Strange and F.W. Pratley, Radionuclides in intertidal sands

And sediments from Morecambe Bay to the Dee estuary. United Kingdom Atomic Energy

Authority Report, AERE-R-13803 (1991).

[16] F.R. Livens and M.S. Baxter, The Sci the Total Environ **70**, 1 (1988).

[17] E.K. Duursma, Ocean Mar Biol: An Annual Review **10**, 137 (1972).

[18] J. Clifton, Relationship between radionuclide activity and sediment composition in Eastern

Irish Sea intertidal sediments. PhD thesis, University of Liverpool (1998).

[19] E. Flint, Natural and anthropogenic controls on saltmarsh accretion history: the Dee estuary,

NW England. B.A. Dissertation, Department of Geography, University of Cambridge, UK

(2007).

[20] R.D. Moore, J. Wolf, A.J Souza and S.S. Flint, Geomorph **103**, 588 (2009).

[21] Rubina Rahman, A.J. Plater, P.J. Nolan, B. Mauz, P.G. Appleby. J. Environ Radioact **119**,

55(2013).

[22] J.A. Hetherington, D.F. Jefferies, Neth. J. sea Res., **8** , 319 (1974).

[23] A. Barbanti and M.H. Bothner, Environ Geol **21**, 3 (1993).

[24] A.B. Cundy and I.W. Croudace, J. of Sedimen Petrol **42**, 102 (1995).

[25] D.J. Assinder, Behaviour of plutonium in the inter-tidal sediments of the eastern Irish Sea

Ecological Aspects of Radionuclide ReleaseP.J. Coughtrey, J.N.B. Bell, T.M. Rob

erts (Eds.), Special Publication No. 3 of the British Ecological Society, British Ecological

Society, Reading, 189 (1983).

[26] M. Vriend and M.A. Prins, Geochem Geophys Geosys **8** (7), 1 (2004).

[27] S.J. Blott,GRADISTAT version 4.0, Package for the analysis of laser granulometer,

Department of Geology, Royal Holloway University of London, UK (2000).

[28] W.C. Krumbein and F.J. Pettijohn, Manual of Sedimentary Petrography, Appleton-Century-

Crofts, New York, N.Y., 549 (1938).

[29] R.L. Folk (1954) . J. Geology **62**, 344 (1954).

[30] R.L. Folk and W.C. Ward, J. Sediment. Petrology **27**, 3(1957)

[31] Q. He and D.E. Walling, J. Environ Radioact **30**, 117 (1996).

[32] T. Allen, (1992). Particle size analysis. In: Stanley-Wood, N.G., Lines, R.W. (Eds.). Royal

Society of Chemistry, UK.

[33] P. G. Appleby, N. Richardson and P.J. Nolan, Nucl Instrum and Meth Phys Res. Section Sec

B: Beam Interactions with Materials and Atoms **71**(2), 228 (1992).

[34] IAEA. Measurements of radionuclides in food and the environment. Vienna: IAEA;

Technical Report Series 295 (1989).

[35] Rubina Rahman et al., Radiat.Prot. Dosim. **154** (4), 477 (2012).

[36] Rubina Rahman and A. Solodov, Health Phys. **111** (5), 465 (2016).

[37] S. Amatullah, Rubina Rahman, J. Ferdous, M.M.M. Siraz, M. U. Khandaker, S.F. Mahal. Int.

J. Environ. Anal. Chem. (2021), https://doi.org/10.1080/03067319.2021.1907361

[38] G.J. Hunt, Radia Protec Dosim **8**, 215 (1984).

[39] Rose, C.L., McKay, W.A., Leonard, D.R.P., Barr, H.M., Toole, J., Halliwell, C.M., Sci. The

Tot. Environ **191**, 1 (1996).

[40] DEFRA CLR interim report, The radioactivity contaminated land exposure assessment

methodology-technical report, January, (2007), http://www.defra.gov.uk

[41] W.A. McKay, P.J.P. Bonnett, H.M. Barr, J.M. Howorth, J. Environ Radioact **21**, 77 (1993).

[42] Rose, C.L., McKay, W.A., Barr, H.M., Toole, J., Halliwell, C.M., 1995. Radioactivity in Two

Tide-washed Marsh Areas in the Eastern Irish Sea: A Radiological Assessment Rep. No.

MAFF RP0401, DOE/HMIP/RR/95/008, DOE/RAS/95/008.

[43] UNSCEAR 2000, Sources and Effects of Ionizing Radiation. United Nations, New York. 453

(2000).

[44] Clifton J., Relationship between radionuclide activity and sediment composition in Eastern

Irish Sea intertidal sediments. PhD thesis, University of Liverpool, (1998).

[45] R.J. Clifton and E.I. Hamilton, Estuar, Coast and ShelF Sci **14**, 433 (1982).

[46] A.B. MacKenzie, G.T. Cook and P. McDonald, J. Environ Radioact **44** (2-3), 275 (1999).

[47] P.J. Coughtrey, D. Jackson, C.K. Jones and M.C. Thorne, Radionuclide distribution and

transport in terrestrial and aquatic ecosystems, volume l. 5 (1984), A.A. Balkema, Rotterdam.

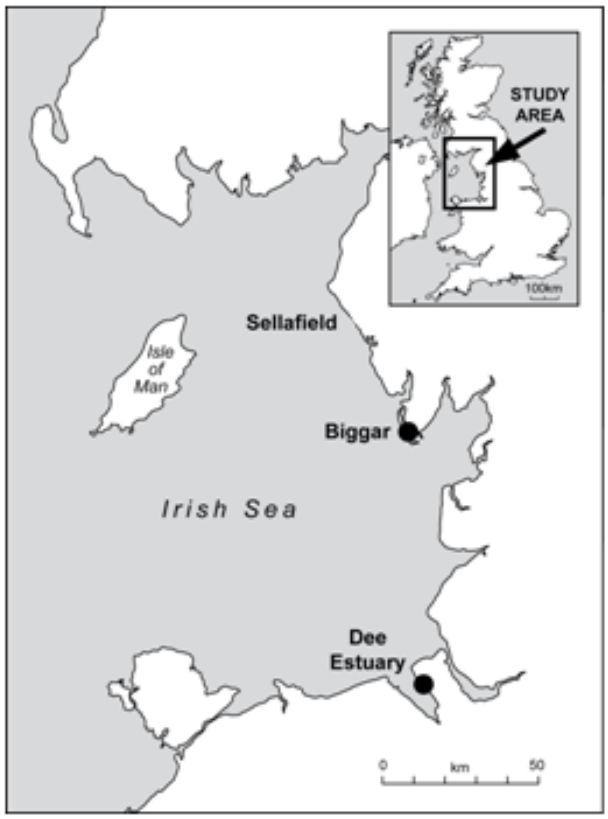

Figure 1: Location map of the Dee and Biggar saltmarsh from the North-West of England, UK.

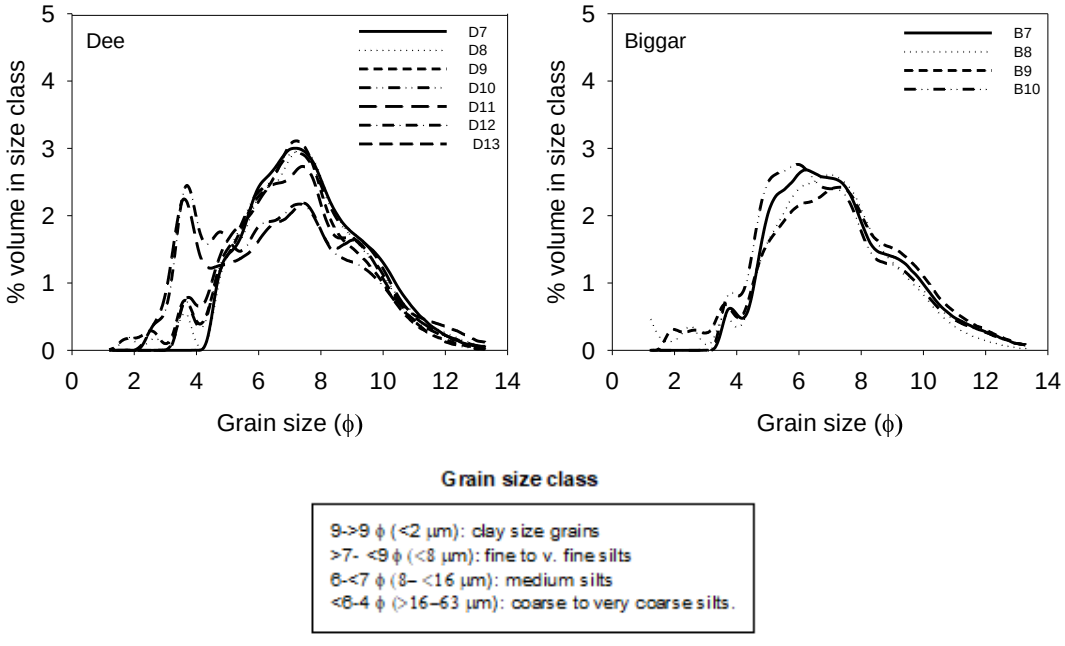

Figure 2: PSDs curves of box core samples (10 cm depth) for size-fractionation from the Dee estuary and Biggar upper saltmarshes.

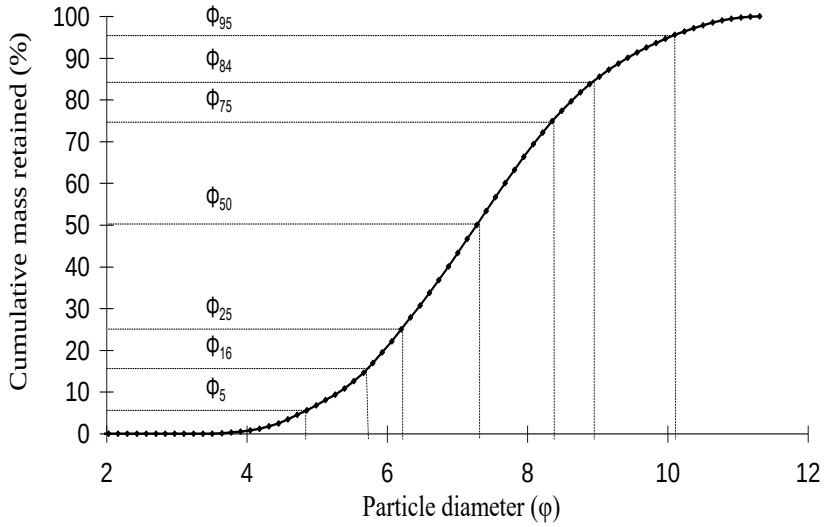

Figure 3. Cumulative frequency curve (an example). φ_n is grain size in phi units at the nth percentage frequency [30].

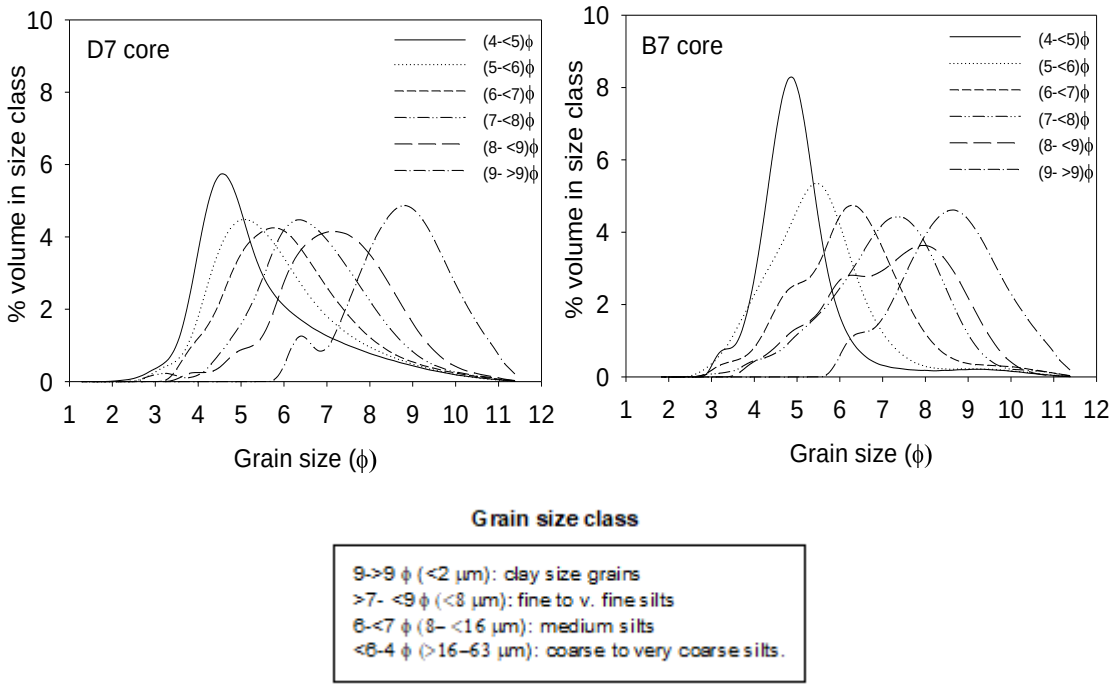

Figure 4: Particle size distributions of size-fractioned samples obtained via gravimetric fractionation of two upper saltmarsh short box core samples from the Dee estuary and Biggar marshes as an example.

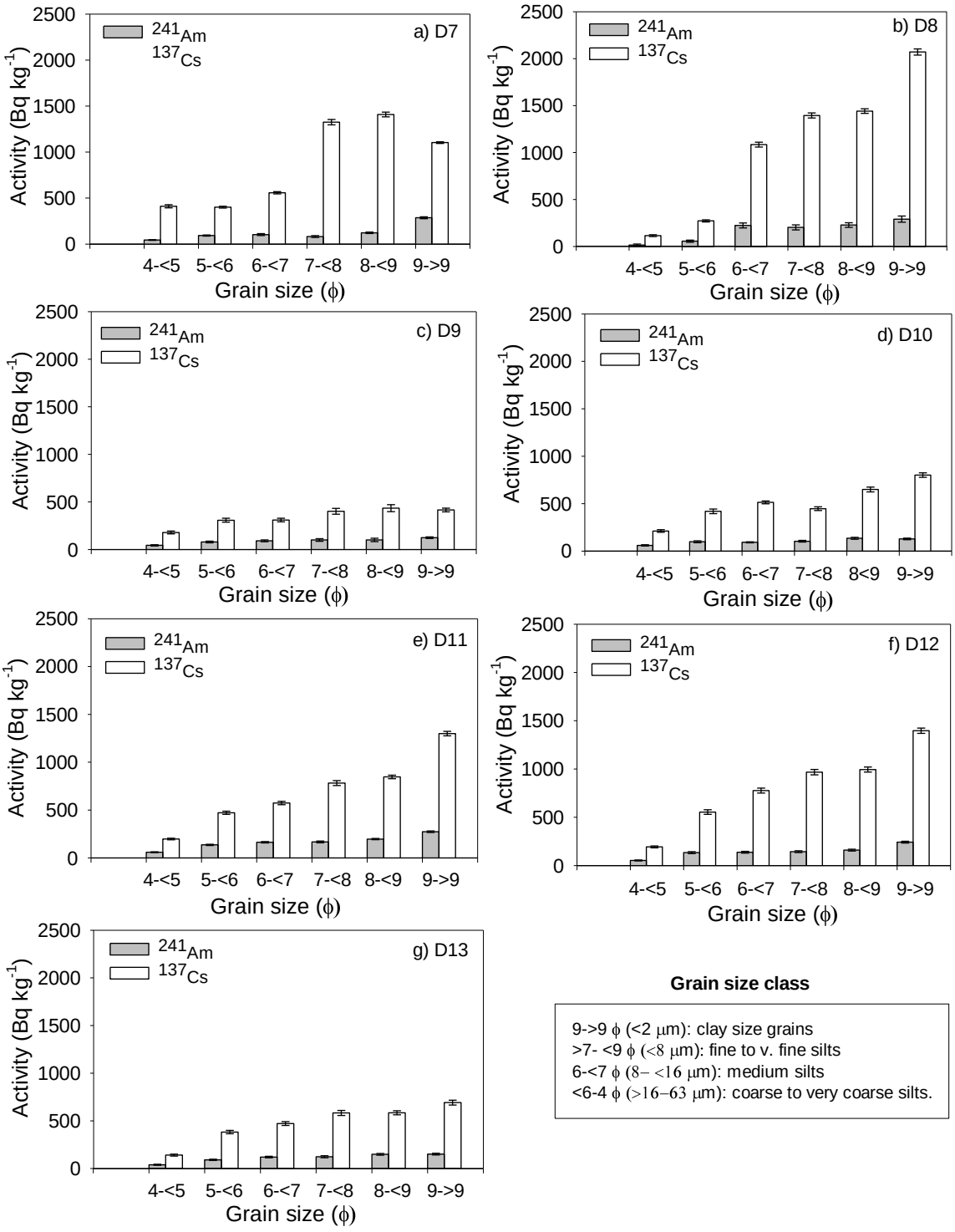

Figure 5: ^{241}Am and ^{137}Cs activities in grain size fractions from the Dee estuary upper saltmarsh short core samples. Error bars represent 2σ counting error.

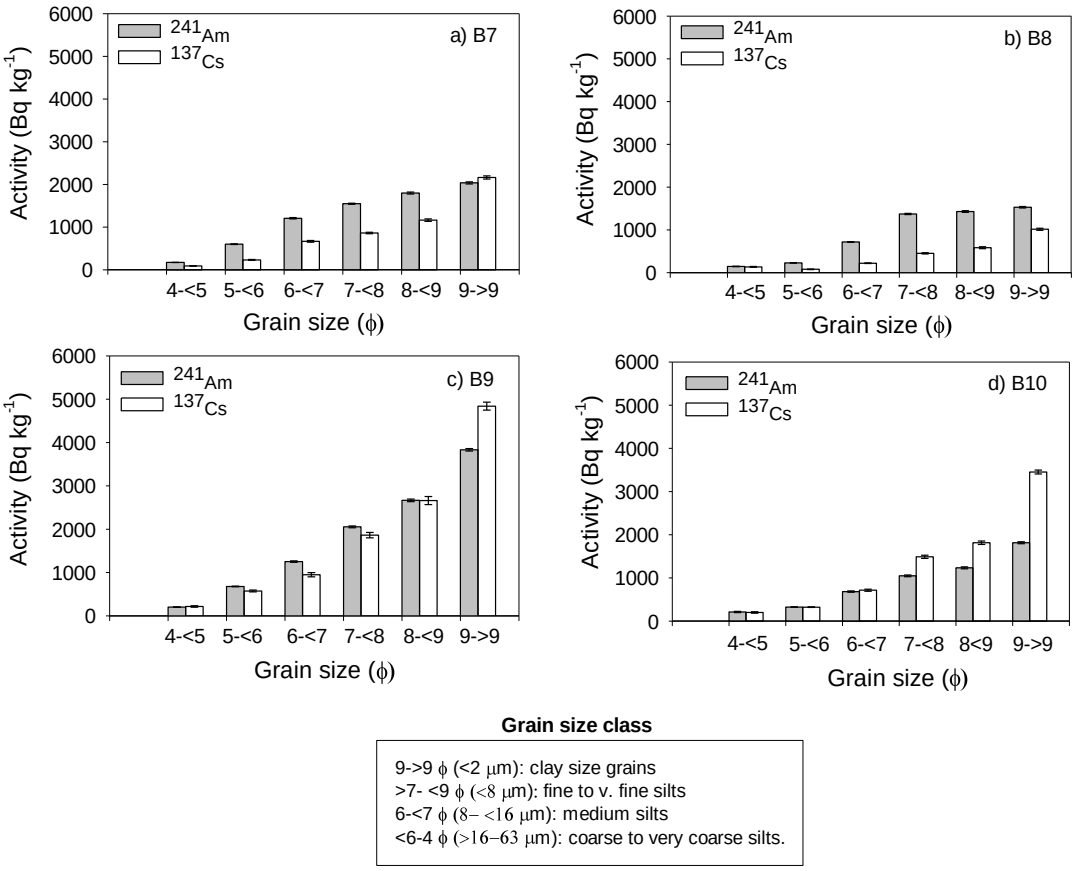

Figure 6: ^{241}Am and ^{137}Cs in grain size fractioned samples from the Biggar upper saltmarsh short core samples. Error bars represent 2σ counting error.

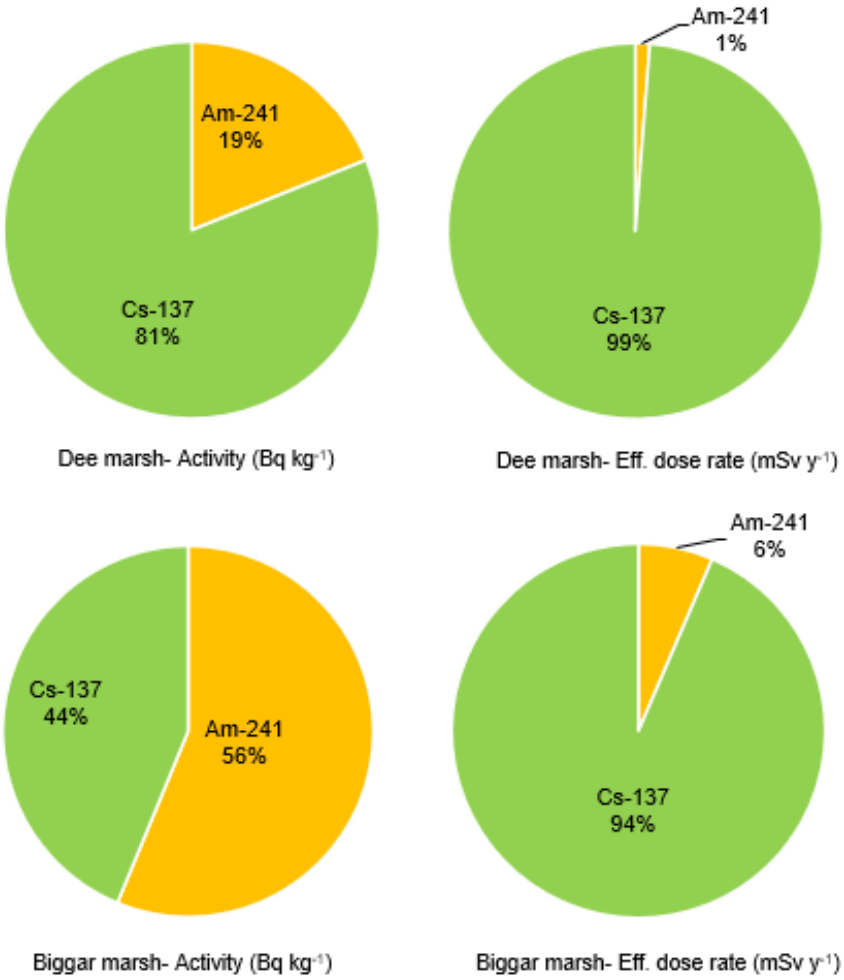

Figure 7: Relative annual outdoor Effective dose distribution due to total ^{241}Am and ^{137}Cs radionuclides contribution in investigated short cores from two sites: 7a-7b) Dee estuary saltmarsh- and 7c-7d) Biggar saltmarsh

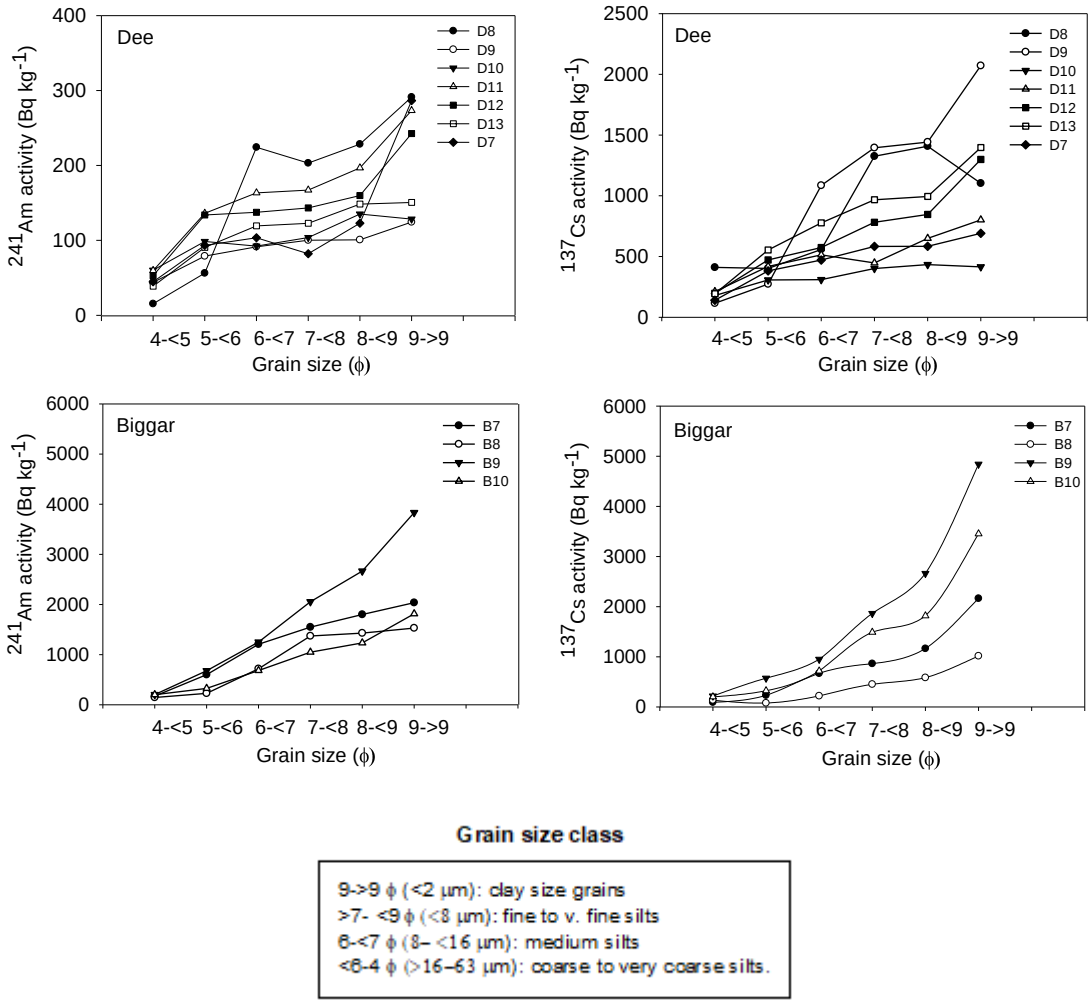

Figure 8: Trend of ^{241}Am and ^{137}Cs in measured grain-size fractions (in phi) from the Dee estuary and Biggar upper saltmarsh short core samples.

Table 1. Radioactivity and grain size characteristics of selected short cores for size fractionation from the Dee estuary and Biggar saltmarshes.

Name of saltmarsh	Core ID	Total Radionuclide activity (Bq kg^{-1})		Textural characteristics		
		^{241}Am	^{137}Cs	% clay	% silt	% sand
Dee estuary	D1	171 ± 3	907 ± 9	22.1	77.9	0
	D2	269 ± 4	1309 ± 10	20.5	75.5	4
	D3	103 ± 3	306 ± 8	16.8	77.1	6.1
	D4	88 ± 4	373 ± 10	18.3	78.4	3.3
	D5	136 ± 2	485 ± 5	21.6	77.0	1.4
	D6	130 ± 3	491 ± 8	19.3	78.4	2.3
	D7	139 ± 3	568 ± 8	21.3	74.8	3.9
Biggar marsh	B1	1531 ± 7	1091 ± 9	19.1	78.3	2.6
	B2	925 ± 4	474 ± 5	15.3	78.1	6.6
	B3	2581 ± 4	1980 ± 5	21.1	71.8	7.1
	B4	1293 ± 6	1383 ± 9	17.0	79.2	3.8

Table 2. Activity concentrations in measured size fractions from the Dee estuary saltmarsh short cores. Data in ( ) show the mean % abundance of total sample volume of corresponding size-fractions.

Name of saltmarsh & Radionuclide	Core ID	^{241}Am and ^{137}Cs activity (Bq kg^{-1}) in grain size fractions (micron class)						Average ^{241}Am & ^{137}Cs, (Bq kg^{-1})	Average ^{241}Am & ^{137}Cs, (Bq kg^{-1})	Average ^{241}Am & ^{137}Cs (Bq kg^{-1})
		63 - >31 *μm*	31 - >16 *μm*	16 - >8 *μm*	8 - >4 *μm*	4 - >2 *μm*	2 - <2 *μm*	Very coarse to coarse silts (63 - >16 *μm*)	Medium to fine silts (16 - >8 *μm*)	Fine silts to clay (8 - <2 *μm*)
Dee estuary										
^{241}Am	D1	45 ± 7	93 ± 4	103 ± 5	82 ± 9	123 ± 9	286 ± 4	69 (10%)	103 (21%)	164 (20%)
	D2	15 ± 2	56 ± 2	224 ± 5	203 ± 5	228 ± 4	**291 ± 5**	36 (10%)	224 (20%)	241 (19%)
	D3	44 ± 3	79 ± 4	91 ± 5	100 ± 7	101 ± 9	124 ± 4	61 (11%)	91 (20%)	108 (17%)
	D4	60 ± 3	99 ± 5	92 ± 3	104 ± 4	135 ± 5	128 ± 4	79 (11%)	92 (20%)	122 (18%)
	D5	60 ± 2	136 ± 3	163 ± 4	167 ± 5	197 ± 3	273 ± 4	98 (10%)	163 (14%)	212 (16%)
	D6	53 ± 2	134 ± 5	137 ± 5	143 ± 5	160 ± 5	243 ± 5	93 (13%)	137 (15%)	182 (14%)
	D7	41 ± 2	101 ± 4	138 ± 4	168 ± 3	149 ± 3	191 ± 5	71 (12%)	138 (19%)	169 (18%)
^{137}Cs	D1	411± 17	402 ± 10	558 ± 13	1326 ± 29	1408 ± 25	1103 ± 9	407 (10%)	558 (21%)	1279 (20%)
	D2	115 ± 5	273 ± 6	1085 ± 13	1395 ± 14	1442 ± 12	**2071 ± 16**	194 (10%)	1085 (20%)	1636 (19%)
	D3	179 ± 7	307 ± 10	310 ± 9	401 ± 15	434 ± 18	415 ± 10	243 (11%)	310 (20%)	417 (17%)
	D4	211 ± 7	419 ± 12	513 ± 7	447 ± 10	649 ± 13	801 ± 12	315 (11%)	513 (20%)	633 (18%)
	D5	197 ± 4	472 ± 8	574 ± 9	782 ± 13	846 ± 9	1299 ± 12	335 (10%)	574 (14%)	976 (16%)
	D6	193 ± 5	554 ± 12	777 ± 13	967 ± 14	994 ± 13	1397 ± 14	373 (13%)	777 (15%)	1119 (14%)
	D7	174 ± 4	424 ± 10	654 ± 10	949 ± 10	953 ± 9	1452 ± 17	299 (12%)	654 (19%)	1118 (18%)

Table 3. Radionuclide activity concentrations in measured size fractions from the *Biggar saltmarsh* selected core samples. Data in ( ) show the mean % abundance of total sample volume of corresponding size fractions.

Name of saltmarsh & Radionuclide	Core ID	^{241}Am and ^{137}Cs activity (Bq kg^{-1}) in grain size fractions (micron class)						Average ^{241}Am & ^{137}Cs, (Bq kg^{-1})	Average ^{241}Am & ^{137}Cs, (Bq kg^{-1})	Average ^{241}Am & ^{137}Cs (Bq kg^{-1})
		63 - >31 *µm*	31 - >16 *µm*	16 - >8 *µm*	8 - >4 *µm*	4 - >2 *µm*	2 - <2 *µm*	Very coarse to coarse silts (63 - >16 *µm*)	Medium to fine silts (16 - >8 *µm*)	Fine silts to clay (8 - <2 *µm*)
Biggar										
^{241}Am	B1	172 ± 1	600 ± 5	1208 ± 8	1548 ± 7	1799 ± 11	2036 ± 12	386 (14%)	1208 (21%)	1794 (17%)
	B2	**144 ± 3**	227 ± 3	717 ± 4	1372 ± 7	1429 ± 10	1529 ± 9	**186** (13%)	717 (21%)	1443 (16%)
	B3	203 ± 3	678 ± 4	1251 ± 8	2054 ± 10	2665 ± 15	**3832 ± 14**	**441** (12%)	**1251** (18%)	**2850** (17%)
	B4	212 ± 4	326 ± 2	683 ± 8	1048 ± 10	1234 ± 11	1815 ± 11	269 (17%)	**683** (19%)	**1366** (15%)
^{137}Cs	B1	92 ± 2	232 ± 5	668 ± 10	862 ± 9	1163± 14	2163 ± 19	162 (14%)	668 (21%)	1396 (17%)
	B2	135 ± 5	**78 ± 3**	220 ± 4	451 ± 7	583 ± 11	1015 ± 12	**107** (13%)	**220** (21%)	**683** (16%)
	B3	217 ± 4	573 ± 5	949 ± 12	1864 ± 16	2661 ± 23	**4840 ± 23**	**395** (12%)	**949** (18%)	**3122** (17%)
	B4	200 ± 3	323 ± 4	716 ± 12	1488 ± 18	1816 ± 20	3453 ± 22	262 (17%)	716 (19%)	2252 (15%)

Table 4a: Annual outdoor external effective dose data of total radionuclide mean activity for all investigated short cores from the Dee estuary and Biggar upper saltmarsh samples.

Site name	Core ID	Total Activity range ^{241}Am (Bq kg^{-1})	Mean Activity ^{241}Am (Bq kg^{-1})	Mean external Eff. dose rate range, ^{241}Am (mSv y^{-1})	Mean external Eff. dose rate ^{241}Am (mSv y^{-1})	Total Activity range ^{137}Cs (Bq kg^{-1})	Mean Activity ^{137}Cs (Bq kg^{-1})	Mean external Eff. dose rate range, ^{137}Cs (mSv y^{-1})	Mean external Eff. dose rate ^{137}Cs (mSv y^{-1})
Dee estuary saltmarsh	D1-D7	88-269	**148**	0.001-0.002	**0.001**	306-1309	**634**	0.03-0.08	**0.05**
Biggar saltmarsh	B1-B4	925-2581	**1583**	0.01-0.02	**0.01**	474-1980	**1232**	0.06-0.15	**0.11**

Table 4b: Annual outdoor external effective dose data from mean activity of particle size fractioned (PSF) samples (63-< 2 µm) for all investigated short cores from the Dee estuary and Biggar upper saltmarsh samples.

Site name	Core ID	PSF samples Activity range, ^{241}Am (Bq kg^{-1})	Mean Activity ^{241}Am (Bq kg^{-1})	Mean external Eff. dose rate range, ^{241}Am (mSv y^{-1})	Mean external. Eff. dose rate, ^{241}Am (mSv y^{-1})	PSF samples Activity range, ^{137}Cs (Bq kg^{-1})	Mean Activity ^{137}Cs (Bq kg^{-1})	Mean external Eff. dose rate range, ^{241}Am (mSv y^{-1})	Mean external Eff. dose rate ^{137}Cs (mSv y^{-1})
Dee estuary saltmarsh	D1-D7	36-224	**117**	0.001-0.0013	**0.001**	194-1636	**658**	0.005-0.01	**0.06**
Biggar saltmarsh	B1-B4	186-2850	**1050**	0.03-0.08	**0.01**	107-3122	**911**	0.05-0.11	**0.08**

Table 5. Textural characteristics data of particles size distribution within the short core samples from the upper Dee Estuary (D1-D7) and Biggar (B1-B4) saltmarshes selected for PSF analysis in the range from 63 to <2 μm (indicated in bold letters).

Core ID	**D1**	**D2**	**D3**	**D4**	**D5**	**D6**	**D7**	**B1**	**B2**	**B3**	**B4**
Textural group	Mud	Mud	Mud	Mud	Sandy Mud	Sandy mud	Mud	Mud	Mud	Mud	Mud
Mean grain size	Fine Silt	Fine Silt	Fine Silt	Fine Silt	Medium Silt	Medium Silt	Fine Silt	Fine Silt	Medium Silt	Fine Silt	Medium Silt
% gravel	0.0%	0.0%	0.0%	0.0%	0.0%	0.0%	0.0%	0.0%	0.0%	0.0%	0.0%
% sand	0.0%	4.0%	6.1%	3.3%	16.7%	16.5%	3.9%	2.6%	6.6%	7.1%	3.8%
% mud	**100.0%**	**96.0%**	**93.9%**	**96.7%**	**83.3%**	**83.5%**	**96.1%**	**97.4%**	**93.4%**	**92.9%**	**96.2%**
% medium sand	0.0%	0.7%	0.8%	0.0%	0.0%	0.0%	0.0%	0.0%	1.8%	0.9%	0.0%
% fine sand	0.0%	0.9%	1.6%	0.0%	2.8%	2.3%	0.0%	0.0%	1.9%	2.2%	0.0%
% v fine sand	0.0%	2.4%	3.7%	3.3%	13.8%	14.2%	3.9%	2.6%	2.8%	4.0%	3.8%
% v coarse silt	5.4%	5.1%	6.8%	7.0%	9.7%	12.8%	8.6%	8.7%	8.1%	8.2%	12.5%
% coarse silt	14.5%	14.0%	14.6%	15.2%	10.9%	12.3%	14.8%	19.0%	17.0%	15.1%	20.4%
% medium silt	20.9%	19.5%	20.3%	20.2%	14.3%	15.0%	18.7%	20.6%	20.6%	17.6%	19.2%
% fine silt	21.7%	21.8%	21.7%	21.2%	15.6%	15.6%	19.5%	18.2%	19.5%	17.9%	16.5%

% v fine silt	15.4%	15.2%	13.6%	14.9%	12.0%	10.9%	13.3%	11.9%	13.0%	12.9%	10.5%
% clay	22.1%	20.5%	16.8%	18.3%	20.7%	16.9%	21.3%	19.1%	15.3%	21.1%	17.0%

Table 6. Rank correlation coefficients (normal font) and significance levels (Italic font) of % abundance with radionuclide activity and Loss on Ignition (LOI, as a proxy for organic carbon) of corresponding measured grain size fractions for Dee estuary and Biggar saltmarsh short core samples.

Saltmarsh name	Grain size φ *(μm)* / Radionuclide & LOI	% 4-<5 φ *(63->31)*	% 5- <6 φ *(31->16)*	% 6- <7 φ *(16->8)*	% 7- <8 φ *(8->4)*	% 8- <9 φ *(4->2)*	% 9- >9 φ *(2-<2)*
Dee estuary	^{241}Am	0.54 *(0.18)*	- 0.40 *(0.34)*	- 0.70 *(0.07)*	- 0.18 *(0.66)*	- 0.29 *(0.49)*	0.57 *(0.15)*
	^{137}Cs	0.14 *(0.72)*	- 0.36 *(0.39)*	- 0.43 *(0.30)*	0.11 *(0.78)*	0.36 *(0.39)*	0.11 *(0.78)*
	LOI	- 0.11 *(0.78)*	- 0.29 *(0.49)*	**0.93** ***(2 × 10^{-7})***	0.46 *(0.26)*	0.36 *(0.39)*	0.11 *(0.78)*
Biggar	^{241}Am	0.40 *(0.75)*	-0.40 *(0.75)*	-0.32 *(0.75)*	0.32 *(0.75)*	0.63 *(0.33)*	2 *(0.08)*
	^{137}Cs	0.00 *(1.00)*	-0.20 *(0.92)*	-0.95 *(0.08)*	-0.63 *(0.33)*	-0.11 *(0.92)*	0.80 *(0.33)*
	LOI	-0.20 *(0.92)*	0.60 *(0.42)*	-0.32 *(0.75)*	0.32 *(0.75)*	0.11 *(0.92)*	- 0.40 *(0.75)*